# Design of a Needle Insertion Module for Robotic Assisted Transperineal Prostate Biopsy

**C. Vaida[1], I. Birlescu[1*], N. Plitea[1], N. Crisan[2], D. Pisla[1]**

[1]*CESTER, Technical University of Cluj-Napoca, Romania, e-mail:*

*{calin.vaida, iosif.birlescu.nicolae.plitea, doina.pisla }@mep.ucluj.ro*

[2]*University of Medicine and Pharmacy, e-mail: drnicolaecrisan@gmail.com*

**Abstract**. The paper presents the design of a needle insertion module for robotic assisted transperineal prostate biopsy, using a commercially available biopsy gun. The module is designed to be used as an end-effector for different robotic systems suitable for this medical task. The geometric and kinematic parameters of the insertion module are presented in correlation with a set of experimental data that supplied critical inputs for the solution development.

**Key words:** Needle insertion module, transperineal prostate biopsy, transrectal ultrasound, biopsy gun.

# 1 Introduction

Prostate cancer is the most commonly diagnosed form of cancer among men, and one of the leading causes for cancer-related deaths in both Europe and USA, with over 220.000 cases predicted and over 25.000 fatalities for 2015 in USA [1, 2]. Diagnosis and treatment methods for this pathology usually consist of: prostate specific antigen (PSA) analysis and biopsy which serve as a diagnosis method and brachytherapy (i.e. radioactive seed placement inside the tumor volume) for therapy. Prostate needle interventions use specialized needles: on one hand, for biopsy the needle is designed for sampling tissue from the prostate gland; on the other hand, for brachytherapy the needle is designed to deliver the radioactive seeds within the tumor volume.

With the advance in the medical robotics since the end of 20th century more and more solutions for needle placement are found in the literature [3, 4]. The motivation for robotic assisted needle placement, guided with different methods of medical imaging, lies in the fact that robots can exceed the human limitations (e.g. accuracy, undesired movement, natural tremor) [4, 5]. Currently, three medical

* Corresponding author

imaging methods exist for robotic assisted needle placement, each with distinct advantages and disadvantages [5]: transrectal ultrasonography (TRUS), computerized tomography (CT), and magnetic resonance (MR) imaging. TRUS is the "golden standard" imaging method for prostate biopsy due to the fact that is cost effective and widely available. However, TRUS offers limited precision, with biopsy sensitivity between 60 and 85% [5] and sometimes the patient needs to be rebiopsied due to false negative results [5]. CT and MR imaging solves the precision limitations of TRUS due to high tissue contrast and high volumetric resolution. However, both CT and MR methods have their limitations: the ionizing radiation dose received by the patient and/or clinician during the procedure duration for CT guided needle placement, and robot design challenges for MR guided interventions (i.e. due to the high magnetic field magnetic components are prohibited, and metal components should be used with increased care since they introduce noise in the MR image) [4, 5].

Increased effort was made in the past 30 years in the scientific community to develop reliable robotic models for prostate interventions [4]. From all the proposed models in the literature, only a few are selected to highlight the current state of the art in robotic assisted needle placement with applications in prostate biopsy.

Gang Li et al presented a robotic model with 6 DoF (3 Cartesian DoF for needle position, and 3 DoF for needle driving module) for transperineal prostate biopsy [6]. The robot is MRI compatible, is designed to use standard biopsy needles, and offers needle rotation in the insertion stage. Krieger A et al developed a series of APT-MRI (Access to Prostate Tissue under MRI guidance) robotic systems designed for transrectal biopsy. APT-I and APT-II contains a manually actuated 3 DoF needle guidance module (2 DoF for the needle translation and rotation, and 1 DoF for the needle insertion) [7, 8]. In contrast with the manually actuated needle guiding approach from APT I and APT II, the needle guiding module from APT-III is designed with 2 motor actuated DoF for needle position and manually (1 DoF) needle insertion [9]. Staianovici et al developed MrBot, a fully actuated MRI compatible robot with 4 DoF for transperineal prostate interventions. MrBot uses pneumatic stepper actuators designed for MRI compatibility [10]. Fichtinger G. et al presented a robotic structure with 6 DoF designed for transperineal prostate biopsy under CT guidance [11].All the above mentioned robotic systems, with their associated needle insertion modules, have their distinct characteristics; however none of them are designed for automatically needle insertion and firing of a biopsy gun after the insertion. To our best knowledge there are no modules that are able to perform this operation using commercially available biopsy guns. The study in this paper is focused on developing a fully actuated needle guiding module with 2 DoF (1 DoF for needle insertion/retraction, and 1 DoF for gun firing) for transperineal prostate biopsy using the BARD™ Monopty 22 mm biopsy gun [13]. The needle guiding module is designed to be integrated into the BIO-PROS1 parallel structure presented in [14, 15], to perform automated transperineal prostate biopsy guided by TRUS imaging).

# 2 Clinical characteristics

Prostate cancer is a progressive disease with metastatic risk correlated with the tumor size. Research shows that metastasis can only appear in tumors with volume greater than 4 mL [9, 12]. A tumor volume of 0.5 mL was proposed for clinical relevance for prostate cancer [9]. Assuming a tumor volume of 0.5 mL, with a spherical shape, the resulted tumor diameter will be 9.8 mm [9]. Krieger A. et al reports in [5] that a needle placement target accuracy of 5 mm or better is desired for prostate biopsies guided with MR imaging.

The prostate gland is about 40x30x30 mm in size, and it is localized under the bladder, completely surrounding the proximal part of urethra. Depending on the thickness of the subcutaneous tissue the prostate is localized at 70 ± 20 mm behind the perineum tissue [9].

The most common used screening method for prostate cancer is the prostate-specific antigen test (PSA), which measures the blood concentration of PSA to estimate the likelihood of prostate cancer. However this method alone can’t accurately determine the presence of prostate cancer. Therefore a biopsy is required (usually 12-18 cores are removed) if the PSA levels are higher than normal, to determine the cancer presence and the degree of its extension [9].

The current “golden standard” for prostate biopsy is the TRUS guided needle biopsy i.e. the biopsy needle is inserted in the gland trough the wall of the rectum. An alternative way for prostate biopsy is the transperineal approach, i.e. the needle is inserted in the gland through the perineum tissue. The disadvantage of this approach, in comparison with the transrectal biopsy, is the longer needle insertion path, and more patient discomfort. However, the transperineal approach offers some advantages that determined the scientific community to explore this method: i) it eliminates the risk of infection (that is up to 5%) present in TRUS biopsy; ii) it eliminates other possible TRUS complications (acute urinary retention and clot retention), iii) it provides the sampling possibility of the entire prostate volume (the apex being impossible to reach transrectally) [17].

The needle guiding module described in this study is designed to work, guided by the BIO-PROS-1 parallel robotic structure [14,15,16]. BIO-PROS-1 has two parallel modules, one for the needle guidance and one for the TRUS probe guidance [14,15,16]. Designed to be used for transperineal prostate biopsy, the BIO-PROS -1 robotic system has to synchronize the two robotic arms, positioning the TRUS probe always below the needle guiding device. The TRUS probe will be inserted inside the patient through the rectum while the needle will be inserted through the perineum, the two entry points being located at a distance between 30 and 50 mm apart on the vertical axis, depending on the size of the patient. The structure, presented in Fig. 1 consists of two modules connected together: the first is a parallel module with 3 DOF with three active joints ($q_1$, $q_2$, $q_3$) which are translational along axes parallel with the OY ($q_1$), respectively OZ ($q_2$, $q_3$) of the fixed frame of the robot, generating the positioning of the mobile platform with constant orientation in space. The second module is a 3 DOF module working in cylindrical coordinates, having two active translational joints ($q_4$, $q_5$). The mobile platforms of the two modules are connected using two Cardan joints. The robotic arm which drives the needle insertion module has a similar configuration of the modules as the first arm, but with both modules placed on the same side of the robotic system, (Fig. 1).

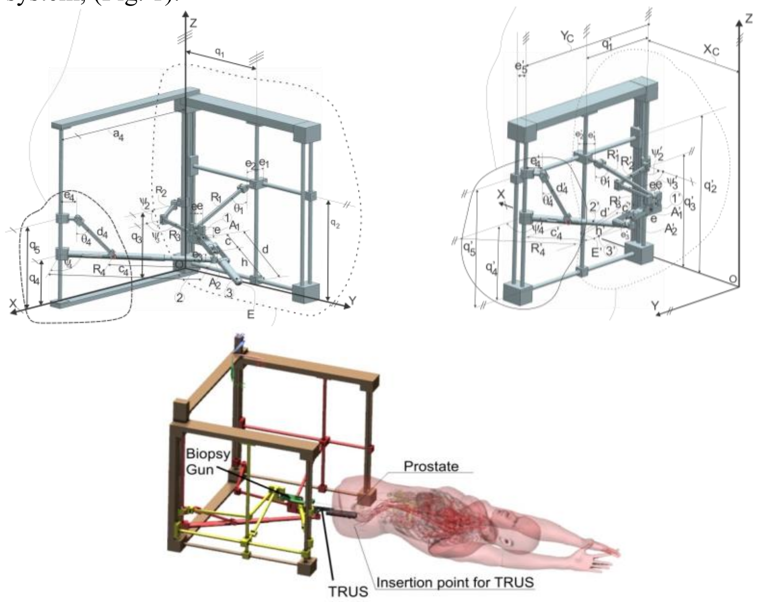


Fig 1. BIO-PROS 1: TRUST guiding module on the top left; needle insertion module on the top right; virtual model within medical environment [15]

A protocol for automated prostate biopsy is presented in [6], and it is extended in this paper (Fig. 2) for transperineal prostate biopsy under TRUS guidance:

1. The robot (BIO-PROS-1) is initialized and the module is moved in home position.
2. The robot positions the module to a predefined needle position and orientation, i.e. the module is moved from the home position and the needle is aligned with the insertion point.
3. The needle is inserted through the perineum tissue, on a linear trajectory, into the prostate gland until the target point is reached.
4. The biopsy gun is fired leading to a quick actuation of the stylet (a) followed by quick actuation of the cannula (b) in order to capture the target tissue inside the needle (see Fig. 2).
5. The needle is retracted from the patient (linear trajectory).
6. The module is moved back to the home position

After the biopsy is completed, following the above mentioned protocol, the biopsy gun is removed from the guiding module, the tissue is collected, the biopsy gun is placed back on the module, and the procedure is repeated until all the tissue samples are collected.

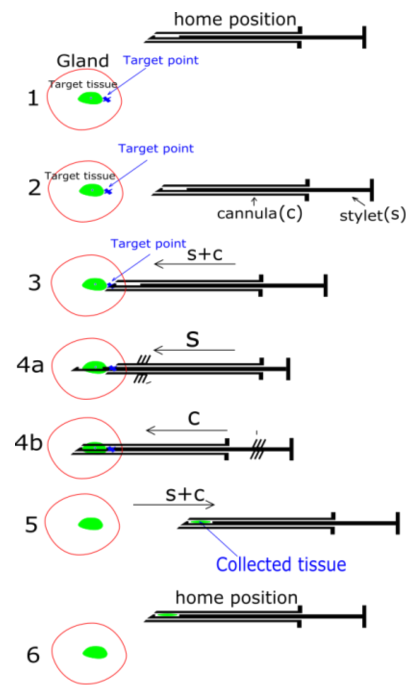


Fig. 2. Protocol for robotic assisted prostate biopsy using a biopsy gun.

# 2 Model design

The needle insertion module is designed to work with the BIO-PROS-1 parallel structure but it can be adapted with minimal modifications to work with any robot which can perform the necessary motions for the transperineal biopsy of the prostate. For transperineal prostate biopsy the patient is placed in a gynecologic position, therefore the TRUS probe will operate under the biopsy gun. By taking this into consideration, the needle insertion module should be designed with increase care on using components in its lower part, to avoid collisions with the TRUS probe. Therefore the actuator is fixed on top of the module and the translation mechanism on the side, as it is described further in this section.

The needle insertion module works with the BARD Monopty 22mm biopsy gun (Fig. 3), which contains a biopsy needle with the back side encapsulated into a plastic handle with a rotating sleeve that is used to load the gun, and a circular button behind the handle to fire the biopsy gun. The gun loading procedure is done in a sequence having two steps: by rotating the sleeve counter-clockwise about 180° the needle cannula gets retracted by about 18 mm (after this step the biopsied tissue is collected from the needle), and next, by rotating the sleeve counter-clockwise another 180° the stylet is retracted by 18 mm. The gun loading sequence is performed manually by the clinician, which does not impose any disadvantage since the biopsied tissue has to be collected from the gun anyway.

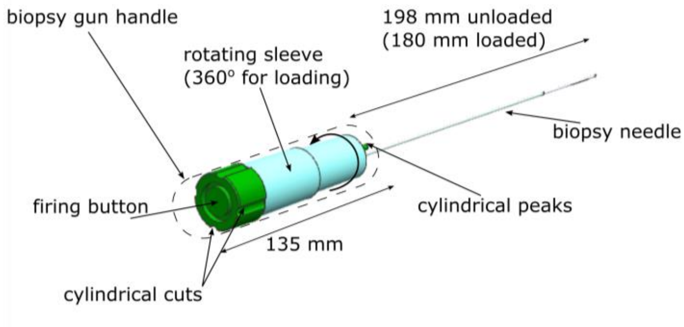


Fig 3. CAD illustration of the biopsy gun.

Referring to the robot characteristics and the operating specifications above mentioned, designing a needle insertion module to work with the BARD Monopty 22mm biopsy gun is feasible. The module should have three main components namely: a platform that is linked with the robot, a mobile (relative to the fixed platform) support that holds the biopsy gun, and a needle tip holder.

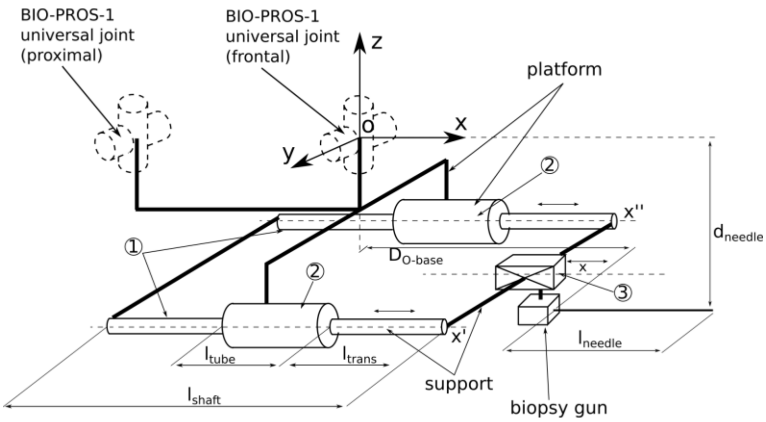


Fig. 4. Conceptual scheme of the needle insertion module

The linkage between the fixed platform and the biopsy gun support is described in Fig. 4. The Cartesian coordinate system is fixed on the platform of the module into a point desired for the connection with the BIO-PROS-1 parallel robot (this will make it easy to relate the needle insertion module to the robot coordinate system). Therefore the center of the chosen coordinate system and the center of the universal joint from the frontal part of the end effector (for the biopsy needle) are equivalent (see Fig. 4).The needle axis is parallel to the OX axis and lies in the XOZ plane at distance $d_{needle}$. The linkage between the platform and the mobile support is created via two parallel passive cylindrical joints (using the shaft (1) from the support and the bushings (2) from the platform). This will ensure the translation motion that will insert the needle on the linear trajectory inside the patient body.

The shaft length ($l_{shaft}$) and the tube length ($l_{tube}$) permit a total translation ($l_{trans}$) of the support (and needle):

$$0 \le |l_{trans}| \le l_{shaft} - l_{tube} \tag{1}$$

As the shafts slide through the bushings $l_{trans}$ varies, i.e. if the shafts are translated along X' and X'' axes (parallel to OX) allowing the motion in both directions, i.e. the insertion and retraction of the needle.

The needle tip has the coordinates:

$$\begin{pmatrix} x_{nt} \\ y_{nt} \\ z_{nt} \end{pmatrix} = \begin{pmatrix} x_{nt} \\ 0 \\ d_{needle} \end{pmatrix} \tag{2}$$

Where $x_{nt}$ can be determined as following:

$$x_{nt} = l_{needle} + l_{trans} + d_{st} \tag{3}$$

Where $d_{st}$ is the distance in along the X axis from the origin O and the proximal part of the needle when translation is minimum (i.e .zero in our case) and it can be computed from:

$$d_{st} = d_{O-base} - l_{trans} \tag{4}$$

Where $d_{O\text{-}nbase}$ is the distance (X coordinate) from O to the needle base (the proximal part). Finally the needle tip coordinates are obtained:

$$\begin{pmatrix} x_{nt} \\ y_{nt} \\ z_{nt} \end{pmatrix} = \begin{pmatrix} l_{needle} + l_{trans} + d_{st} \\ 0 \\ d_{needle} \end{pmatrix} \tag{5}$$

The linear motion is obtained through the active prismatic joint (3) which is actuated along the Xt axis (parallel to OX) using a screw/nut mechanism.

The CAD design of the needle insertion module and its components, developed in Siemens NX, are presented in Fig. 5. The biopsy gun support has a fixed part (4) and a revolving part (5) (around R axis parallel to OX) to allow an open/close sequence to place and fix the biopsy gun. The pistol is placed into the mobile part (5) of the support and then the support is closed by pushing it up against the fixed part (4) and locking the two parts together via a screw mechanism (6). The biopsy gun handle has a design with four cylindrical partially cuts in the back side and two cylindrical peaks in the front side (see Fig. 3). The support design takes advantage of these geometric features, and with a back cover (7), it ensures a reliable fixed position of the pistol when the support is closed. On the left and right side of the support there are cylindrical shafts (1), which create cylindrical joints with the fixed platform. On the top there is a platform (8) (parallel to XOZ plane) with a carving in which a ball nut (3) is fixed to create the translation mechanism. The firing mechanism is simply a spindle drive (9) fixed into a support (10) placed and fixed behind the back cover (7) of the fixed support part (4).

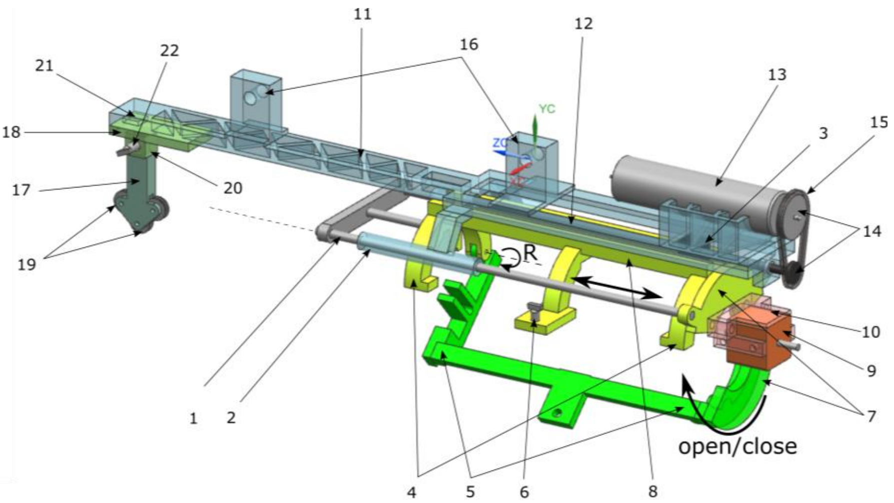


Fig. 5. CAD illustration of the needle insertion module with its highlighted components.

The platform (11) (lying on a plane parallel to OXZ) is connected with the pistol support via two cylinder tubes (2) which in combination with the cylindrical shafts (1) from the support creates two parallel cylindrical joints. The translation motion of the support relative with the fixed platform is made with a rotating ball screw (12) (connected with the nut (3)) rotated by the motor (13) through a gear mechanism with two cogwheels (14) and a rubber belt (15).Two extensions (16) are fixed to the platform, in the same plane, to connect the needle insertion module with the BIO-PROS-1 parallel robot.

The needle tip holder (17) is connected in the frontal part of the fixed platform (11) via a sliding sledge (18). The holder has a mechanism designed with three grooved wheels (19) with spinning axes parallel with OY. The sledge purpose is to allow the motion of the holder along an axis parallel to the needle axis, motion that is needed when the clinician mounts the gun into the support. I.e. the holder must be moved away from the gun when the pistol is being mounted, and moved back after the support is closed so the needle goes through the holder. The holder is removable from the sledge for sterilization related issues. The holder (17) is fixed into its plug (20) using a magnet (21) for exact positioning and a screw (22) for stiffness. The needle holder is fixed relative to the insertion point, and the biopsy needle slides through it in the insertion stage. The wheel mechanism reduces friction in comparison with a fixed needle holding mechanism, which helps especially on the pistol firing stage when the needle velocities are high. The space between the wheels is 1.6 mm i.e. the mechanism is designed for the standard 1.6 mm diameter biopsy needles found within the Monopty 22mm biopsy gun.

For a needle insertion correlated with the clinical specifications presented in section 2, the length of the cylindrical shafts is chosen 175 mm while the length of the cylindrical counterparts from the platform is 60 mm. This offers a total of 115 mm translation of the needle tip, which allows certain flexibility in determining the needle distance relative to the insertion point, and allows the reach of the target point from various needle positions and orientations.

The total mass of the needle insertion module is:

$$m_{\text{module}} = m_{fix} + m_{move} \tag{6}$$

Where $m_{\text{fix}}$ is the mass of the parts that are not actuated by the modules motor (platform, needle holder, motor), and $m_{\text{move}}$ is the mas of the motor actuated parts (support, biopsy gun, firing mechanism).

The formula needed to calculate the thrust generated when torque is applied is:

$$F_a = \frac{2\pi \cdot \eta 1 \cdot T}{Ph} \tag{7}$$

With:

| | |
|---|---|
| $F_a =$ | Thrust generated by the torque (N); |
| $Ph =$ | Feed screw lead (mm); |
| $\eta 1 =$ | Positive efficiency of the feed screw (%); |
| $T =$ | Driving torque (Nmm). |

$F_a$ can be viewed as the frictional resistance on the guided surface (i.e. friction inside the cylindrical joints of the module):

$$F_a = \mu \cdot m_{move} \cdot g \tag{8}$$

Assuming perfect surface contact in the cylindrical joints, and taking into account the tissue resistance on needle insertion, using Equation (7) the net thrust when torque is applied is defined as:

$$F_{total} = F_a + F_{tissue} \tag{9}$$

Where $F_{tissue}$ = tissue resistance.

The torque needed to maintain a linear motion (constant velocity) of the biopsy gun in the insertion stage is:

$$T = F_{total} \cdot \frac{Ph}{2\pi \cdot \eta 1} \tag{10}$$

The torque needed to accelerate the needle has to be computed by accounting all the moments of inertia of the rotating parts:

$$T_{acc} = J \cdot \dot{\omega} \tag{11}$$

Where:

$J$ – total moment of inertia ($kg \cdot m^2$)

$\dot{\omega}$ – angular acceleration ($rad \cdot sec^{-2}$)

The total moment of inertia is calculated from:

$$J = m_{move} \cdot \left( \frac{P}{2 \cdot \pi} \right)^2 + J_s + J_a + J_b \tag{12}$$

Where:

$J_s$ – moment of inertia of the screw

$J_a$ – moment of inertia of the gear attached to the screw

$J_b$ – moment of inertia of the gear attached to the motor shaft

$$J_a = J_b = m_{pul} \cdot d^2 \cdot \frac{1}{8} \tag{13}$$

Where:

$m_{pul}$ – mass of the pulleys from the gear (10 grams)

$d$ – outer diameter of the pulleys (15 mm)

The angular acceleration can be calculated from:

$$\dot{\omega} = \frac{d(2 \cdot \pi \cdot N)}{dt} \tag{14}$$

With:

$N$ – number of rotations per sec

The tissue resistance was experimentally determined using ex vivo animal tissue (pig leg) as a test sample (Fig. 6). The needle was inserted into the tissue using the ZWICK/ROELL testing equipment that has a 24 bit measured-value resolution and an acquisition rate of 2 kHz. The reactive force was continuously registered. The results obtained from 5 experimental trials, as well as the mean of those trials are presented in Fig. 6 for biopsy needle insertion, with and without skin incision. The point of insertion was carefully selected not to be closer than 5 mm than the previous insertion point to avoid following a needle path that was already used, therefore measuring lower forces since the tissue was already penetrated. However with this approach it is easy to observe the variations in the force curve since the needle, most likely, penetrated trough different tissue (fat, muscle etc.) for every experimental trial. The velocity during needle insertion was 10 mm/sec and the force was registered for 8 sec. This leaves a variable interval of depth length of about 70 mm. As illustrated in Fig. 7, the resulted tissue resistance to needle insertion was in less than 10 N.

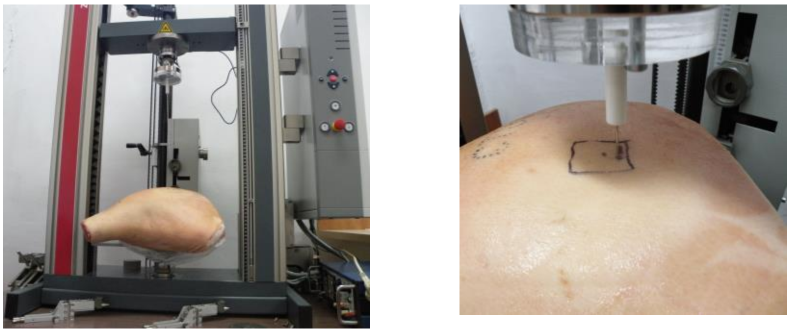

Fig. 6. Tissue resistance on needle insertion experimental setup. Overview on the left; close view on right.

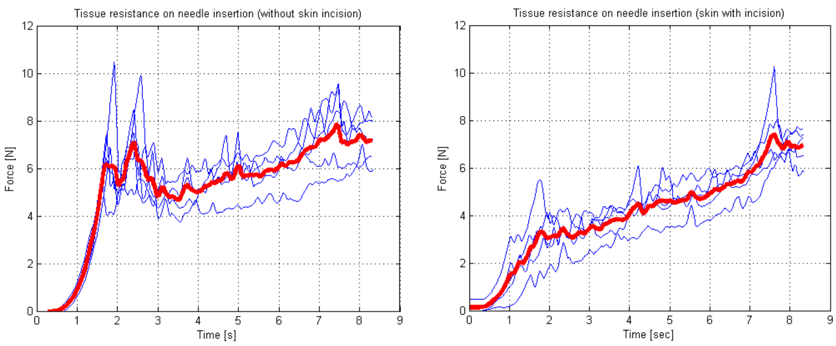


Fig. 7. Reported tissue resistance for needle insertion using ex vivo animal tissue without skin incision (on the left) and with skin incision (on the right).

The experimental results validated also a medical variation of the transperineal procedure performed by specialists from the European Institute of Oncology, Italy, which perform a small incision in the perineum skin and insert the needle in a cone shape through a single port, rather than using parallel trajectories [18]. With this approach, where a skin incision was performed, the resistance force of the tissue has a more linear evolution, eliminating the spike which appear when the skin is penetrated which leads to an increased accuracy due to the elimination of the needle deflection. This approach eliminates the use of a guiding template making the manual needle insertion somewhat more difficult, but using a robotic arm for the needle guidance this drawback is eliminated. Simulation using Siemens NX™ software showed a mass of the mobile parts of the needle insertion module ≈ 175 grams (using Al 5086). The biopsy gun mass is ≈ 50 grams, and by considering the nut and the spindle drive masses, the total moving mass of the module is ≈240 grams. The friction coefficient in the cylindrical joints is 0.04 (steel to teflon since teflon bushings are used inside the joints). By using equation (9) the torque value required for needle insertion (at constant velocity) of ≈ 0.0017 Nm is obtained. Using equations (11-14), with the screw moment of inertia ≈ $0.0285 \cdot 10^{-6}$ ($kg \cdot m^2$), the pulleys moments of inertia ≈ $0.2813 \cdot 10^{-6}$, the required needle velocity =10 $mm \cdot sec^{-1}$ and acceleration =10 $mm \cdot sec^{-2}$ (thus the acceleration time is 1 sec), and finally the rotational velocity 10 $rot \cdot sec^{-1}$, the extra torque required for accelerating motion is obtained ≈ $37.52 \cdot 10^{-6}$ Nm.

The force needed to fire the biopsy gun was experimentally determined by pressing the loaded biopsy gun firing button against a force sensor FSR® from Interlink Electronics™, while the data was acquired using National Instruments™ hardware (NI USB-6210) and MatLab™ software (Fig. 8). The experimental bench was developed inside CESTER research center. Output data from 31 experimental trials showed a normal distribution with a mean of 2.689 V (at gun firing instance) and a standard deviation of 0.11. The force sensor was calibrated using standardized weights to determine the characteristic curve that describes volt to force conversion (Fig. 8). Out of this curve, a force of 7.84 N resulted to be de mean value at the gun firing instance.

An electromagnet or a spindle drive that offers a force of 10 N is recommended since it gives an extra ≈ 25% interval to ensure the gun firing. In the selection of the actuation solution weight is a critical parameter which has to be minimized.

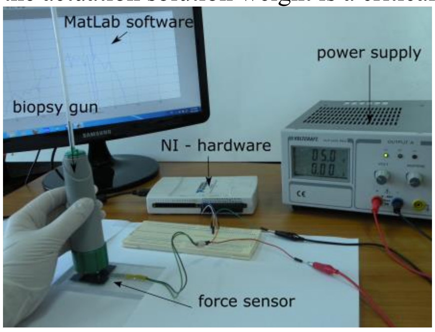


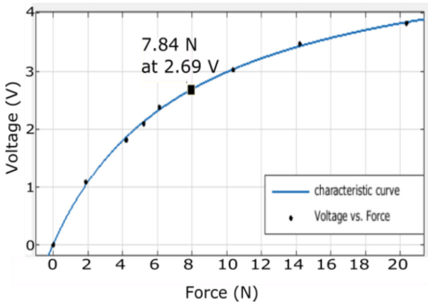


Fig. 8. Experimental setup for the gun firing needed force (left). Voltage to force characteristic curve of the force sensor (right).

Following the above results (calculated and experimentally determined) the proposed actuators (motor and spindle drive) for the needle insertion module and the screw/nut mechanism are the following:

- The Spindle Drive GP 6 S Ø6 mm from Maxon Motor™; max continuous force of 10 N, max intermittent force 18 N, with a mass of 4 grams.
- The motor, ECX SPEED 8 M Ø8 mm, and the planetary gearhead GPX 8 Ø8 mm from Maxon Motor™; offer continuous torque of 0.008 Nm and a maximum intermittent torque of 0.012 Nm with a mass of 9 grams.
- The ball screw and the ball nut from THK, screw model MDK 0401-3 with its afferent nut. The mechanism has the lead of 1 mm, efficiency of 0.95 and it works well at a rotating speed of 600 RPM. The mass of the screw is 10.15 grams while the mass of the nut is 10 grams.

The total mass of the needle insertion module with the biopsy gun mounted is around 560 grams. The compact solution proposed for the needle insertion module makes this device suitable for a wide variety of biopsy procedures, extending its utilization to other organs as well: liver, kidneys, breast, and thyroid. The overall size makes this device also capable of performing CT-Sim guided biopsies, working as the end-effector of a robotic arm which works inside the gantry of the imaging device, such the PARA-BRACHYROB robot [19]. The modular design allows, with minimal changes its conversion towards another biopsy gun, imposing as a single restriction the presence of the release mechanism at the end of the proximal head of the medical instrument.

# 4 Conclusions

This paper presents a needle insertion module for transperineal prostate biopsy designed for the BIO- PROS-1 parallel robot. The module has 2 DoF, one for needle insertion/retraction, and another for gun firing and its parameters reflect its intended purpose. I.e. the total linear translation of the needle allows the reach of the entire prostate gland volume from various points of insertion and needle orientations, while the force provided by the actuators is sufficient for a reliable needle insertion and biopsy gun firing.

Further research is proposed to optimize the needle insertion module (mostly to increase the needle placement accuracy). These optimizations can be either architectural (e.g. placing the needle holder on the correct position by measuring the axial stress along the needle to determine where the needle is more likely to bend in the insertion stage) or structural (e.g. reducing various components mass to move the center of mass on the needle axis). These optimizations are intended to reduce the needle deflection, therefore, as specified, increasing the needle target accuracy.

**Acknowledgments** This paper was realized within the Partnership Programme in priority domains - PN-II, which runs with the financial support of MEN-UEFISCDI through the Project no 59/2015, code PN-II-RU-TE-2014-4-0992 - ACCURATE and Project no. 247/2014, code PN-II-PT-PCCA-2013-4-0647 - ROBOCORE.

# References


1. Siegel, R. Miller, K.: Cancer statistics, CA Cancer J Clin, 2015;65:5–29.
2. Ferlay, J. Steliarova-Foucher E.: Cancer incidence and mortality patterns in Europe: estimates for 40 countries in 2012, Eur J Cancer, 2013;49:1374–1403.
3. Tarun, K. P. et al : AAPM and GEC-ESTRO guidelines for image-guided robotic brachytherapy: Report of Task Group 192, Am. Assoc. Phys. Med., 2014.
4. Stoianovici, D. et al: “MRI Stealth” robot for prostate interventions, Minim Invasive The Allied Technol, 2007 ; 16(4): 241–248.
5. Kriger, A. et al: Design of a Novel MRI Compatible Manipulator for Image Guided Prostate Interventions, IEEE Trans Biomed Eng, 2005 February ; 52(2): 306–313.
6. Li Gang et al: A Fully Actuated Robotic Assistant for MRI-Guided Prostate Biopsy and Brachytherapy. Proc SPIE Int Soc Opt Eng. 2013 Mar 12;8671:867117.
7. Krieger, A. et al: Design of a novel MRI compatible manipulator for image guided prostate interventions. IEEE Trans Biomed Eng. 2005 Feb;52(2):306-13.
8. Krieger, A. et al: An MRI-compatible robotic system with hybrid tracking for MRI-guided prostate intervention. IEEE Trans Biomed Eng. 2011 Nov;58(11):3049-60. doi: 10.1109/TBME.2011.2134096.
9. Krieger, A. et al: Development and Evaluation of an Actuated MRI-Compatible Robotic System for MRI-Guided Prostate Intervention. IEEE ASME Trans Mechatron. 2012 Sep 12;18(1):273-284. Epub 2011 Oct 17.
10. Stoianovici, D. et al: "MRI Stealth" robot for prostate interventions. Minim Invasive Ther Allied Technol. 2007;16(4):241-8. Erratum in: Minim Invasive Ther Allied Technol. 2007;16(6):370.
11. Fichtinger, G. et al: System for Robotically Assisted Prostate Biopsy and Therapy with Intraoperative CT Guidance. Acad Radiol. 2002 Jan;9(1):60-74.
12. Tokuda, J. et al: Preclinical evaluation of an MRI-compatible pneumatic robot for angulated needle placement in transperineal prostate interventions. Int J Comput Assist Radiol Surg. 2012 Nov;7(6):949-57.
13. C. R. Bard, Inc: http://www.bardbiopsy.com/products/monopty.php. Last accessed on 30.01.2016.
14. Plitea, N., Pisla, D., Vaida, C., Gherman, B., Tucan, P., Govor, C., Covaciu, F., Family of innovative parallel robots for transperineal prostate biopsy, Patent pending: A/00191/13.03.2015
15. Pisla, D. et al: On the Kinematics of an Innovative Parallel Robotic System for Transperineal Prostate Biopsy. 14th World Congress in Mechanism and Machine Science, Taipei, Taiwan, 25-30 October, 2015.
16. Pisla, D. et al: Graphical Simulation System for Functional Analysis of a Parallel Robot for Transperineal Prostate Biopsy. Applied Mechanics and Materials ISSN: 1662-7482, Vol. 823, pp 101-106
17. Huang, S. et: Significant impact of transperineal template biopsy of the prostate at a single tertiary institution. Urol Ann. 2015 Oct-Dec;7(4):428-32.
18. Cobelli, O., et al. Predicting Pathological Features at Radical Prostatectomy in Patients with Prostate Cancer Eligible for Active Surveillance by Multiparametric Magnetic Resonance Imaging, PLoS ONE 10(10):e0139696. doi:10.1371/journal.pone.0139696
19. Vaida, C., Pisla, D., Schadlbauer, J., Husty, M., Plitea, N., Kinematic Analysis of an Innovative Medical Parallel Robot using Study parameters, New Trends in Medical and Service Robots: Human Centered Analysis, Control and Design, 2016 (in press)